Production of autoionizing states by double-electron capture in intermediate-energy C^{4+} + He collisions

D. L. Guo,[1,2] R. T. Zhang,[1,2] X. L. Zhu,[1,2] Y. Gao,[1,2] D. M. Zhao,[1,2] K. Z. Lin,[3,1] X. B. Zhu,[1,2] S. F. Zhang,[1,2] and X. Ma[1,2,*]

[1]*Institute of Modern Physics, Chinese Academy of Sciences, Lanzhou 730000, China*
[2]*University of Chinese Academy of Sciences, Beijing 100049, China*
[3]*Hefei National Laboratory for Physical Sciences at Microscale and Department of Modern Physics, University of Science and Technology of China, Hefei, Anhui 230026, China*

(Received 1 September 2022; accepted 6 December 2022; published 3 January 2023)

We have performed a kinematically complete experiment for state-selective double-electron capture occurring in 15-keV/u C^{4+} + He collisions by means of cold-target recoil-ion momentum spectroscopy. It was shown that capture into ground and low excited states of the C^{2+} ions is overwhelmingly dominant. Besides, a small fraction of autoionization decays from doubly excited states of symmetric as well as asymmetric electron configurations following endothermic double-electron capture were clearly observed. Emphasis was given to the population mechanisms of the different electron configurations. Our analysis indicates that electron-electron correlation effects may play a major role in the double-electron capture process. In addition, the large transverse recoil-ion momentum of symmetric configurations as compared to asymmetric configurations for the doubly excited autoionizing states may be attributed to the different number of steps involved in the primary capture process, with the former likely produced by a two-step mechanism and the latter by a one-step mechanism.

DOI: 10.1103/PhysRevA.107.012801

I. INTRODUCTION

Charge-transfer processes occurring in ion-atom collisions have been extensively studied both experimentally and theoretically for several decades. The interest in these processes stems not only from fundamental aspects but also from their importance in various applied fields such as astrophysics and fusion plasma physics [1]. For the most dominant reaction involved in the process, i.e., single electron capture (SEC), one may consider that the essential features are now well understood. However, the situation is quite different for double- or multiple-electron capture, in which the electron-electron correlations may play a decisive role.

Starting from the 1980s, many experiments have been performed for double-electron capture (DEC) occurring in collisions between highly charged ions and neutral targets in the kiloelectronvolt range [2–7]. It was found that in these collisions the two electrons are usually captured into highly excited orbitals, giving rise to the population of doubly excited states of the projectile ion. These states can either radiatively decay (true double capture, TDC) or autoionize by emission of an Auger electron (autoionizing double capture, ADC), thereby resulting finally in an apparent one-electron capture process called transfer ionization. Note that in many cases ADC is dominant and only a few doubly excited states decay via photon emission.

Intuitively, one may speculate that the DEC process leads to the population of symmetric or quasisymmetric doubly excited states due to high selectivity of the electron populations for the SEC process [6]. However, it was found that asymmetric configurations are also important in many cases [3]. Of great interest is the different production mechanisms of symmetric and asymmetric electron configurations. In particular, the mechanisms for the population of asymmetric configurations have been the center of considerable discussion in the literature for many years. Experimentally, the production mechanisms were mostly investigated by means of Auger electron spectroscopy [2,3,8,9] and cold-target recoil-ion momentum spectroscopy (COLTRIMS) [6,7,10]. Study of the production mechanisms using energy gain spectroscopy [11] or photon spectroscopy [12] has been reported as well, but only for a few cases. In parallel, considerable theoretical efforts using the classical curve crossing model [6–8,11,13,14], classical over-barrier model (CBM) [15], Landau-Zener model [4], and in some exceptional cases even more elaborate close-coupling calculations [6] have been devoted to the formation mechanisms of doubly excited states for ADC. Different mechanisms have been proposed to describe DEC, among which the most popular ones are simultaneous correlated double capture (CDC) [16], correlated transfer excitation (CTE) [4,16,17], successive independent two-step process [18], and autotransfer to Rydberg states (ATR) [19]. While the considerable progress represents a large step forward over early efforts, the production mechanisms of DEC are still under debate.

In the present work, the state-selective ADC and TDC processes, resulting finally in apparent one- and two-electron capture channels, respectively, were measured with COLTRIMS for 15-keV/u C^{4+} + He collisions. Contrasting with

*x.ma@impcas.ac.cn

most previous measurements using COLTRIMS which were limited to the measurements of recoil ion only, in this work both the recoil ion and the electrons are measured in coincidence for ADC, which allows to determine the state populations and the corresponding scattering angles of the doubly excited states with either symmetric or asymmetric configurations. Also note that for the endothermic reactions as ADC occurring in C^{4+} + He collisions studied here, the cross sections are much smaller than those of the exothermic reactions which have been the focus of most of the previous work [15,20–26]. By measuring both the recoil ions and the electrons simultaneously, the relatively smaller ADC contribution can thus be identified without serious contamination from other processes. The study of this system is of considerable interest because it gives information on the mechanisms responsible for DEC in endothermic reactions which are energetically forbidden within classical approximation. In addition to the ADC channels, other DEC contributions (e.g., ground and low excited states capture) were briefly discussed in comparison with previous sophisticated quantum mechanical calculations for completeness.

Atomic units (a.u.) are used throughout unless otherwise indicated.

II. EXPERIMENTAL SETUP

The experiment was carried out with a COLTRIMS reaction microscope [27,28] mounted on a 320-kV platform for multidisciplinary research with highly charged ions at the Institute of Modern Physics, Lanzhou. The details of the COLTRIMS have been described elsewhere [29,30]. Briefly, the C^{4+} ions produced in the 14.5-GHz electron cyclotron resonance (ECR) ion source were extracted, charge analyzed, and accelerated to the desired energy. The C^{4+} beam was then transported toward the target chamber and collimated using two sets of adjustable slits to a size of about 1 mm in diameter in the collision zone. Several sets of electrostatic deflectors upstream from the target chamber were used to clean charge state impurities from the beam and to steer the beam to the target.

In the target chamber, the C^{4+} beam crosses a two-stage differentially pumped supersonic gas jet beam produced by the supersonic expansion of He gas through a 30-μm nozzle. The recoil ions and electrons created in the collisions were extracted perpendicular to the incoming C^{4+} beam by a homogeneous electrostatic field and then traveled through field-free drift tubes. Two position-sensitive detectors located at the ends of the drift tubes were used to detect the ions and electrons. To reduce the influence of the finite size of the interaction area on the momentum resolution, we used a so-called one-dimensional time focusing geometry for the recoil ions and electrons [31]. A homogenous magnetic field of about 10.0 G generated by a pair of Helmholtz coils was applied parallel to the electrostatic field so that a much larger solid angle for electron collection could be covered. At the exit of the target chamber, the primary projectile beam and the scattered projectile ions are charge state analyzed by a dipole magnet. Finally, the primary projectile beam was collected with a Faraday cup, whereas the scattered ions were detected with another time- and position-sensitive detector.

In the present experiment, the recoil ion was recorded in coincidence with the scattered projectile. In the offline data analyzing process, the transfer ionization and the TDC channels could be unambiguously identified by the projectile and recoil-ion final charge states in the two-dimensional spectrum of the time of flight of the recoil ions versus the scattered ion position [29]. For the transfer ionization process, the emitted electron was also recorded. The momentum vectors of both the recoil ions and the emitted electrons were reconstructed from the time of flight and the impact positions on the detectors.

III. RESULTS AND DISCUSSION

The measured longitudinal recoil-ion momentum for the TDC is shown in Fig. 1(a) for 15-keV/u C^{4+} + He collisions. It was found that the two target electrons are predominantly captured into the ground states or low excited states that are below the autoionization threshold. The relative contributions of the main channels were determined using the Gaussian curve fitting method to be 39.0%, 37.0%, and 24.0% for capture into $2s^2$, $2s2p$, and $2p^2$, respectively. The measurements are in good agreement with the recent semiclassical atomic-orbital close-coupling (SCAOCC) calculations [26], which predict that the relative contributions for capture into $2s^2$, $2s2p$, and $2p^2$ are 40.5%, 33.9%, and 25.6%, respectively.

For the two-electron process, one of the most interesting questions is whether electron-electron correlation effects are involved or not. One may expect that the process without electron-electron correlation effects can be, to a large extent, described by independent electron approximation. Within such approximation, the two electrons are captured into two neighboring shells (n, n), $(n, n-1)$, $(n-1, n-1)$ with symmetric or quasisymmetric electron configurations, where n stands for the principal quantum number in which single capture primarily occurs [18]. However, it is recalled that the population of symmetric doubly excited states may also be produced by a process involving electron-electron interactions [9]. Thus, both mechanisms with or without electron-electron correlations may contribute to the production of the symmetric configurations. In contrast to the symmetric configurations, it was widely considered that the independent electron approximation cannot account for capture into doubly excited states with asymmetric configurations [6,8,32]. Electron-electron interaction should play an important role in the formation of asymmetric configurations. For the present C^{4+} + He collision process, no clear conclusion can be drawn from the data concerning the question of whether or not the electronic correlations contribute to the symmetric TDC channels. It is, however, interesting to note that the inadequacy of one-electron models to describe the main electronic processes in C^{4+} + He collisions and the importance of the interelectronic interaction have been demonstrated in an extended investigation by Gao *et al.* [26], which clearly demonstrates that the electronic correlations may also be involved in the formation of the symmetric configurations.

Furthermore, according to the SCAOCC calculations [26], these symmetric configurations are produced via simultaneous exchange of both electrons, which is rather in qualitative agreement with previous investigations [21,24,32]. The

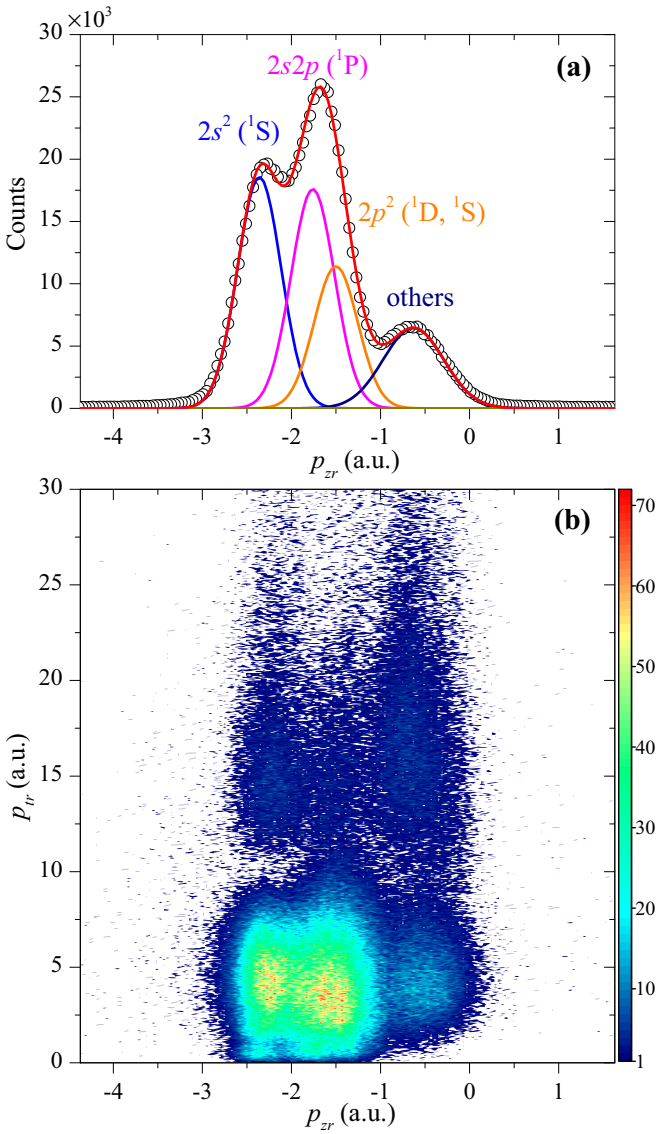

FIG. 1. The measured recoil-ion momentum distribution for TDC for 15-keV/u C^{4+} + He collisions. (a) The longitudinal recoil-ion momentum distribution; (b) the two-dimensional recoil-ion momentum distribution showing the transverse momentum vs the longitudinal momentum of the recoil ion.

transverse recoil-ion momentum might be supportive of the population mechanism. The measured longitudinal versus transverse recoil-ion momentum distribution is shown in Fig. 1(b). It can be seen that the transverse recoil-ion momentum distribution for different populations shows similar features and mainly lies within 8 a.u.. The peaking of the main distributions near a relatively small transverse momentum is roughly consistent with the expectation from a classical model [5,7,11,13,14,27,33], which shows that the two-step mechanism accounts for the large-angle scattering, while the one-step process is mainly responsible for small-angle scattering.

It can be seen from Fig. 1(a) that for C^{4+} + He collisions at the impact energy considered, there is almost no observable contribution of radiative decays from the doubly excited states above the autoionization threshold, indicating that the doubly excited states populated were almost exclusively autoionizing. However, double-electron capture to autoionizing states is strongly suppressed since the involved channels are endothermic [34]. The autoionization decays could be better identified from the measured two-dimensional electron momentum distributions parallel and perpendicular to the projectile beam, as shown in Fig. 2(a). It can be seen that the electrons are emitted preferentially in the forward direction in the laboratory frame. The most noticeable feature is the semicircle patterns of varying sizes centered around the projectile, which is clear proof of an ADC mechanism. Besides, quite a few electrons are found as well in the region between the target and the projectile in Fig. 2(a). The so-called saddle point mechanism [35], a widely discussed mechanism for the direct transfer ionization process, may be responsible for these relatively low-energy electron emissions. According to the mechanism, the emitted electron will be found in the region between the target and the projectile due to the two center effects [36], i.e., the emitted electron moves in the combined Coulomb field induced by the recoil ion and the projectile ion. In the following we focus on the different production mechanisms of the doubly excited states formed in the ADC process.

For ADC, three groups of electron momentum distributions associated with different autoionizing doubly excited states are identified from the distributions, as marked by three semicircular lines in Fig. 2(a). The electron energy in the projectile frame [Fig. 2(b)] clearly shows the characteristic energies of the three groups of ADC electrons, i.e., 0.4 eV, 3.1 eV, and 14.1 eV. According to previous calculated and measured energies of Auger transitions [2], these observed ADC electrons are associated with autoionization following DEC to $1s^2 2p4\ell$, $1s^2 2pn\ell$ ($n \geqslant 5$), and $1s^2 3\ell 3\ell'$, respectively. The contributions for different groups of ADC electrons can be approximately extracted in the two-dimensional correlated spectrum distribution of the electron energy in the projectile frame versus the longitudinal recoil-ion momentum [37], as shown in Fig. 2(c). It can be seen that in the impact energy region of our concern, the contribution of asymmetric configurations is rather large, especially for the $1s^2 2p4\ell$ population, whereas the intensity of the electrons produced from the symmetric DEC is relatively small. Note that electron-electron interaction should play an important role in the formation of asymmetric configurations. It thus appears that the formation of the asymmetric populations $2p4\ell$ and $2pn\ell$ ($n \geqslant 5$) is evidence of electron-electron correlation effects. The large fraction of asymmetric configurations implies the importance of the electron-electron correlations in the ADC process, while the small contribution of the symmetric or quasisymmetric configurations represents an upper limit of the monoelectronic contribution to the process.

As already mentioned above, in addition to the Q-value, the COLTRIMS also gives access to the projectile scattering angle via the measurement of the recoil-ion momentum vector. It has been well established that the scattering angle or transverse momentum exchange can serve to investigate the mechanisms responsible for the process [32]. In Fig. 2(d), the transverse recoil-ion momentum p_{tr} distributions for different ADC contributions selected in Fig. 2(c) are shown. It can be seen that the p_{tr} distribution for symmetric configuration

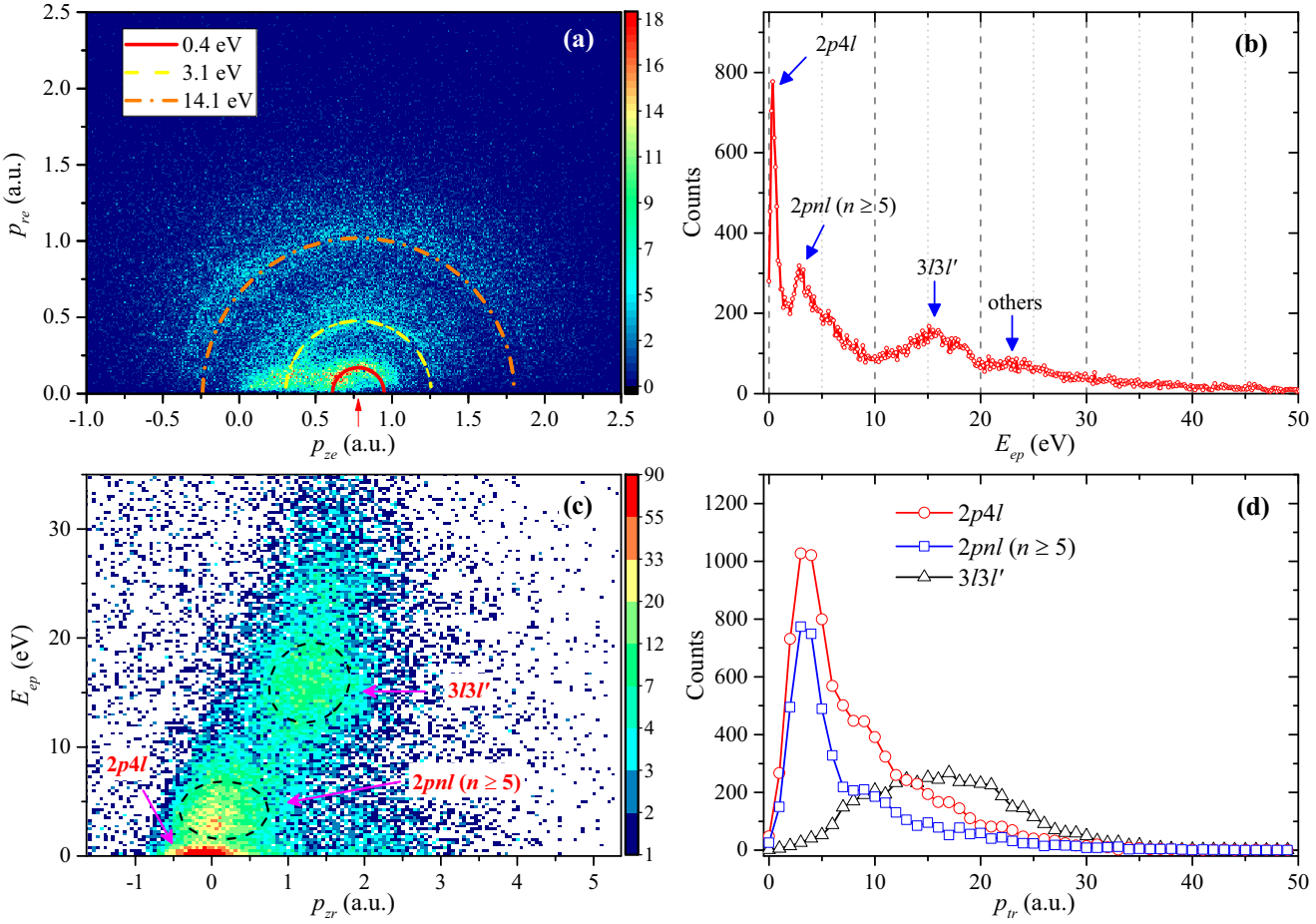

FIG. 2. The measured momentum and energy distributions for transfer ionization for 15-keV/u C^{4+} + He collisions. (a) The two-dimensional electron momentum distributions parallel and perpendicular to the projectile beam; (b) electron energy in the projectile frame; (c) the correlated spectrum of longitudinal recoil-ion momentum vs electron energy in the projectile frame; (d) the transverse recoil-ion momentum. The location of the projectile velocity is indicated by a red arrow in (a).

peaks at 18 a.u., which is about eight times as much as that for asymmetric configuration. The large difference in the p_{tr} distributions for these two configurations indicates that the electron populations of different configurations are related to different capture processes since the followed electron emission does not affect the recoil-ion momentum, which suggests that the formation of asymmetric configurations is not due to the postcollisional effects but rather due to the primary process of the collision. Therefore, the mechanisms proposed based on postcollisional effects such as, for example, the well-known ATR mechanism [19] can be readily excluded, since the ATR mechanism predicts that asymmetric configuration is produced by a transfer process due to configuration interactions with the symmetric configuration formed in the primary capture process. This is in qualitative agreement with the results for ADC in low-energy Ne^{10+} + He collisions [6].

The p_{tr} distributions could also shed light on the number of steps involved in the primary capture process for ADC. One may speculate that the conclusion drawn for exothermic reactions is also justified for the endothermic reactions. In analogy to the exothermic reactions, the much larger deflection for the two-step process could also be attributed to the smaller impact parameters and the longer time spent on Coulomb repulsion for endothermic reactions. Assuming that for endothermic reactions the first and the second step of the two-step process occurs at an internuclear distance of r_{c1} and r_{c2}, respectively, whereas the one-step process takes place at r_c, one might expect that r_{c2} is smaller than r_c, since the charge changed collision partners (C^{3+}, He^+) formed in the first step charge exchange process should come close enough to capture an electron from an He^+ ion by the down-charged projectile C^{3+} ion. More importantly, in order to reach the required internuclear distance for these two mechanisms, the critical (largest) impact parameter for the two-step process should be much smaller than that for the one-step process due to the long-time deflection induced by long-range Coulomb repulsion between the two charge collision partners (C^{3+}, He^+). Therefore, the typical scattering angle for the two-step process can be much larger as compared to the one-step process. From the analysis it thus follows that the emerging large difference of p_{tr} distributions observed in Fig. 2(d) indicates that a two-step DEC process is more likely in symmetric configuration, while a one-step DEC process is preferable in asymmetric configurations. Interestingly, this is different from the above analysis for TDC, where a one-step process is more likely for the symmetric configurations. Clearly, the present analysis concerning the steps involved in the endothermic channels is oversimplified. In order to shed

more insight on the mechanisms, further theoretical efforts beyond the qualitative explanations, as well as extensive kinematically complete experiments, are highly desirable.

IV. CONCLUSION

We have performed a kinematically complete experiment for state-selective double-electron capture occurring in 15-keV/u C^{4+} + He collisions by using COLTRIMS. The true double-electron capture and autoionizing double-electron capture channels have been identified. The results show that capture into the L shell ($2s^2$, $2s2p$, and $2p^2$) is overwhelmingly dominant. Besides the dominant true double-electron capture channels, a small fraction of autoionization decays from doubly excited states of symmetric as well as asymmetric configurations following double-electron capture were observed. Our analysis indicates that electron-electron correlation effects may play a major role in the double-electron capture process. In particular, the minor total cross sections for producing the symmetric or quasisymmetric electron configurations in autoionizing double-electron capture represent an upper limit of the monoelectronic contribution to the process. In addition, for autoionizing double-electron capture, the striking difference of transverse recoil-ion momentum distributions corresponding to different configurations suggests that the electron populations of different configurations are related to different primary capture processes since the subsequent electron emission does not affect the recoil-ion momentum. Moreover, the large transverse recoil-ion momentum of symmetric configurations as compared to asymmetric configurations for the doubly excited autoionizing states may be attributed to the different number of steps involved in the primary capture process, with the former likely produced by a two-step mechanism and the latter by a one-step mechanism. A full theoretical treatment of endothermic double-electron capture processes, as well as further experimental measurements, are required to provide a more refined analysis.

ACKNOWLEDGMENTS

This work was supported by the National Natural Science Foundation of China (Grant No. 11874365), the National Key Research and Development Program of China (Grant No. 2017YFA0402300), and the Strategic Priority Research Program of Chinese Academy of Sciences (Grant No. XDB34020000). D.L.G. is grateful for support from the Youth Innovation Promotion Association of Chinese Academy of Sciences (Grant No. E229111Y). R.T.Z. is grateful for the support from the "Hundred Talents Program" of the Chinese Academy of Sciences. We would like to thank J. W. Gao for helpful discussions.

[1] H. T. Viacheslav Shevelko (eds.), *Atomic Processes in Basic and Applied Physics,* Springer Series on Atomic, Optical, and Plasma Physics Vol. 68 (Springer, Berlin, 2012).
[2] R. Mann, Phys. Rev. A **35**, 4988 (1987).
[3] N. Stolterfoht, C. C. Havener, R. A. Phaneuf, J. K. Swenson, S. M. Shafroth, and F. W. Meyer, Phys. Rev. Lett. **57**, 74 (1986).
[4] F. Fremont, H. Merabet, J. Y. Chesnel, X. Husson, A. Lepoutre, D. Lecler, G. Rieger, and N. Stolterfoht, Phys. Rev. A **50**, 3117 (1994).
[5] H. Laurent, M. Barat, M. N. Gaboriaud, L. Guillemot, and P. Roncin, J. Phys. B **20**, 6581 (1987).
[6] X. Fléchard, C. Harel, H. Jouin, B. Pons, L. Adoui, F. Frémont, A. Cassimi, and D. Hennecart, J. Phys. B: At. Mol. Opt. Phys. **34**, 2759 (2001).
[7] M. A. Abdallah, W. Wolff, H. E. Wolf, E. Y. Kamber, M. Stöckli, and C. L. Cocke, Phys. Rev. A **58**, 2911 (1998).
[8] F. Meyer, C. Havener, R. Phaneuf, J. Swenson, S. Shafroth, and N. Stolterfoht, Nucl. Instrum. Methods Phys. Res., Sect. B **24-25**, 106 (1987).
[9] J.-Y. Chesnel, B. Sulik, H. Merabet, C. Bedouet, F. Frémont, X. Husson, M. Grether, A. Spieler, and N. Stolterfoht, Phys. Rev. A **57**, 3546 (1998).
[10] R. T. Zhang, W. T. Feng, X. L. Zhu, S. F. Zhang, D. L. Guo, Y. Gao, D. B. Qian, S. Xu, S. C. Yan, P. Zhang, Z. K. Huang, H. B. Wang, B. Hai, D. M. Zhao, and X. Ma, Phys. Rev. A **93**, 032709 (2016).
[11] P. Roncin, M. Barat, M. N. Gaboriaud, L. Guillemot, and H. Laurent, J. Phys. B: At. Mol. Opt. Phys. **22**, 509 (1989).
[12] A. Chetioui, F. Martin, M. F. Politis, J. P. Rozet, A. Touati, L. Blumenfeld, D. Vernhet, K. Wohrer, C. Stephan, M. Barat, M. N. Gaboriaud, H. Laurent, and P. Roncin, J. Phys. B: At. Mol. Opt. Phys. **23**, 3659 (1990).
[13] W. Wu, J. P. Giese, Z. Chen, R. Ali, C. L. Cocke, P. Richard, and M. Stöckli, Phys. Rev. A **50**, 502 (1994).
[14] X. Flechard, S. Duponchel, L. Adoui, A. Cassimi, P. Roncin, and D. Hennecart, J. Phys. B: At. Mol. Opt. Phys. **30**, 3697 (1997).
[15] R. Mann and H. Schulte, Z. Phys. D **4**, 343 (1987).
[16] N. Stolterfoht, C. C. Havener, R. A. Phaneuf, J. K. Swenson, S. M. Shafroth, and F. W. Meyer, Phys. Rev. Lett. **58**, 958 (1987).
[17] H. Winter, M. Mack, R. Hoekstra, A. Niehaus, and F. J. de Heer, Phys. Rev. Lett. **58**, 957 (1987).
[18] M. Barat, M. N. Gaboriaud, and P. Roncin, Phys. Scr. **T46**, 210 (1993).
[19] P. Roncin, M. N. Gaboriaud, M. Barat, A. Bordenave-Montesquieu, P. Moretto-Capelle, M. Benhenni, H. Bachau, and C. Harel, J. Phys. B: At. Mol. Opt. Phys. **26**, 4181 (1993).
[20] J. Tan, C. Lin, and M. Kimura, J. Phys. B **20**, L91 (1987).
[21] M. Barat, P. Roncin, L. Guillemot, M. N. Gaboriaud, and H. Laurent, J. Phys. B: At. Mol. Opt. Phys. **23**, 2811 (1990).
[22] J. P. Hansen, J. Phys. B: At. Mol. Opt. Phys. **25**, L17 (1992).
[23] N. Keller, L. R. Andersson, R. D. Miller, M. Westerlind, S. B. Elston, I. A. Sellin, C. Biedermann, and H. Cederquist, Phys. Rev. A **48**, 3684 (1993).
[24] L. F. Errea, B. Herrero, L. Mendez, and A. Riera, J. Phys. B: At. Mol. Opt. Phys. **28**, 693 (1995).
[25] L. L. Yan, Y. Wu, Y. Z. Qu, J. G. Wang, and R. J. Buenker, Phys. Rev. A **88**, 022706 (2013).

[26] J. W. Gao, Y. Wu, N. Sisourat, J. G. Wang, and A. Dubois, Phys. Rev. A **96**, 052703 (2017).
[27] R. Dörner, V. Mergel, O. Jagutzki, L. Spielberger, J. Ullrich, R. Moshammer, and H. Schmidt-Böcking, Phys. Rep. **330**, 95 (2000).
[28] J. Ullrich, R. Moshammer, A. Dorn, R. Dörner, L. P. H. Schmidt, and H. Schmidt-Böcking, Rep. Prog. Phys. **66**, 1463 (2003).
[29] X. Ma, R. T. Zhang, S. F. Zhang, X. L. Zhu, W. T. Feng, D. L. Guo, B. Li, H. P. Liu, C. Y. Li, J. G. Wang, S. C. Yan, P. J. Zhang, and Q. Wang, Phys. Rev. A **83**, 052707 (2011).
[30] X. Ma, X. Zhu, H. Liu, B. Li, S. Zhang, S. Cao, W. Feng, and S. Xu, Sci. China Ser. G-Phys. Mech. Astron. **51**, 755 (2008).
[31] W. C. Wiley and I. H. McLaren, Rev. Sci. Instrum. **26**, 1150 (1955).
[32] M. Barat and P. Roncin, J. Phys. B: At. Mol. Opt. Phys. **25**, 2205 (1992).
[33] P. Roncin, M. Barat, and H. Laurent, Europhys. Lett. **2**, 371 (1986).
[34] N. Stolterfoht, C. Havener, R. Phaneuf, J. Swenson, S. Shafroth, and F. Meyer, Nucl. Instrum. Methods Phys. Res., Sect. B **27**, 584 (1987).
[35] R. Dörner, H. Khemliche, M. H. Prior, C. L. Cocke, J. A. Gary, R. E. Olson, V. Mergel, J. Ullrich, and H. Schmidt-Böcking, Phys. Rev. Lett. **77**, 4520 (1996).
[36] R. Olson, C. Feeler, C. Wood, C. Cocke, R. Dörner, V. Mergel, H. Schmidt-Böcking, R. Moshammer, and J. Ullrich, Nucl. Instrum. Methods Phys. Res., Sect. B **124**, 249 (1997).
[37] L. P. H. Schmidt, F. Afaneh, M. Schöffler, J. Titze, O. Jagutzki, T. Weber, K. Stiebing, R. Dörner, and H. Schmidt-Böcking, Phys. Scr. **T110**, 379 (2004).